Materials Research Letters

ISSN: 2166-3831 (Online) Journal homepage: www.tandfonline.com/journals/tmrl20

Characterization of ripplocation mobility in graphite

J. Gruber, M. W. Barsoum & G. J. Tucker

To cite this article: J. Gruber, M. W. Barsoum & G. J. Tucker (2020) Characterization of ripplocation mobility in graphite, Materials Research Letters, 8:2, 82-87, DOI: 10.1080/21663831.2019.1702115

To link to this article: https://doi.org/10.1080/21663831.2019.1702115

© 2019 The Author(s). Published by Informa UK Limited, trading as Taylor & Francis Group.

View supplementary material

Published online: 15 Dec 2019.

Submit your article to this journal

Article views: 1707

View related articles

View Crossmark data

Citing articles: 9 View citing articles

Full Terms & Conditions of access and use can be found at
https://www.tandfonline.com/action/journalInformation?journalCode=tmrl20

MATER. RES. LETT.
2020, VOL. 8, NO. 2, 82–87
https://doi.org/10.1080/21663831.2019.1702115

ORIGINAL REPORT

OPEN ACCESS

Characterization of ripplocation mobility in graphite

J. Gruber [a], M. W. Barsoum [b] and G. J. Tucker [c]

[a]Materials Science, Colorado School of Mines, Golden, CO, USA; [b]Materials Engineering, Drexel University, Philadelphia, PA, USA; [c]Mechanical Engineering, Colorado School of Mines, Golden, CO, USA

ABSTRACT

Recent work suggests that layered solids deform through buckling of basal planes. When isolated locally, as in graphite, these buckles, termed ripplocations, behave superficially similar to dislocations, but have no Burgers vectors. Through atomistic simulations, we demonstrate the easy transitions of ripplocations in graphite between many closely-spaced energy states, even at low temperatures. Between 60 and 350 K, their migration barrier is estimated at 32 meV, independent of segment length. Ripplocations spontaneously migrate towards vacancies and away from compressive stresses. These results shed more light on this new micromechanism and potentially explain experimental observations that evade sufficient description through dislocation-based models.

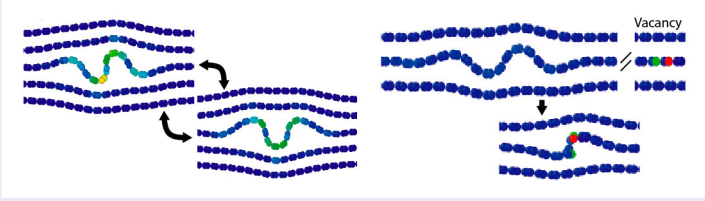

IMPACT STATEMENT

These results shed more light on this new micromechanism and the high mobility and vacancy interactions of ripplocations potentially explain experimental observations that evade sufficient description through dislocation-based model.

ARTICLE HISTORY
Received 26 July 2019

KEYWORDS
Layered solids; deformation mechanisms; buckling; ripplocations

Introduction

Layered solids are common both in nature and modern technologies, with applications including batteries, nuclear materials, and a wide array of electronic devices. The deformation of certain layered solids is confined at least initially to two dimensions, along the basal planes, reflecting the fundamentally structural anisotropy of these materials. This anisotropic plastic deformation has typically been held to depend only on the motion of basal dislocations, BDs [1,2–6]. Recent work, however, suggests that individual atomic planes may buckle in response to mechanical stimulus similarly to systems at orders of magnitude larger length-scales [7]. This elastic buckling phenomenon plays a crucial in the experimentally observed, non-linear elastic, hysteretic mechanical behavior under compression of certain materials, the kinking non-linear elastic, KNE, solids [8,9]. This deformation response has previously been explained through spontaneously reversible dislocation plasticity based on early-work by Frank and Stroh. However, this model fails to account for some properties of the deformation of these materials, such as delamination and c-axis strain [10], which may be explained by including nanoscale elastic buckling. Spatially localized nanoscale buckling has been implicated in graphene [11], graphite [12,13], MoS_2 [8], Ti_3SiC_2 [9], and other materials [14–17], using a variety of terminology for classification and identification. Following work performed on surface ripples in MoS_2 by Kushima et al. [8], we use the term 'ripplocation' to describe this phenomenon. Through Molecular Dynamics, MD, simulation, ripplocations were determined to have neither Burgers vector nor polarity [9]. In graphite, MD simulations demonstrated that ripplocations are attracted to other ripplocations, and in aggregate on many layers spontaneously coalesce into 'ripplocation boundaries', RBs, fully reversible precursors of more

CONTACT G. J. Tucker tucker@mines.edu

Supplemental data for this article can be accessed here. https://doi.org/10.1080/21663831.2019.1702115

© 2019 The Author(s). Published by Informa UK Limited, trading as Taylor & Francis Group.
This is an Open Access article distributed under the terms of the Creative Commons Attribution License (http://creativecommons.org/licenses/by/4.0/), which permits unrestricted use, distribution, and reproduction in any medium, provided the original work is properly cited.

permanent kink boundaries. Simulated nanoindentation parallel to the basal planes showed the formation of multiple RBs beneath the indenter [18]. The fully elastic and energy-dissipative response shows close alignment with experimental indentations performed on KNE solids [19].

Spherical nanoindentation of single crystals with planes directly parallel or normal to the load direction provides a simple test to determine whether a material deforms by BD or by RBs. While in the normal loading case linear elasticity gives way directly to plastic deformation forming smooth and permanent indentation marks, in the latter, at intermediate strains, spontaneous and fully reversible stress–strain curve hysteresis loops are generated in the absence of indentation marks [9,20] At higher stresses, permanent delamination cracks–parallel to the basal planes–form providing unambiguous evidence for c-axis strain. When the indenter is loaded normal to the basal planes on the other hand, at sufficiently high stresses, massive pop-ins result in the accumulation, or buildup, of large pileups at the indentation edges, which is incompatible with continuous plastic deformation associated with BDs. Additionally, BDs cannot produce c-axis strain, which is frequently observed in the deformation of KNE solids. We presented transmission electron microscopy, TEM, evidence for c-axis strain in Ti_3SiC_2 grains that were loaded with a spherical nanoindenter [9]. Very recently, high resolution TEM evidence showed the presence of a large number of nanobridges in a naturally deformed mica [15]. The microstructure was characterized by significant expansion along the c-direction, with a plethora of bridging nanoripples, or nanoribbons, with very high radii of curvature, holding the sample together. Since these observations are not explainable in a BD framework, a different micromechanism or strain accommodation mechanism must be operative. The c-axis strain produced by ripplocations can provide the answer.

A combination of atomistic simulations of graphite and simple instrumented cylindrical indentation experiments on various layered materials—plastic cards, thin steel, and Al sheets—showed that in all cases, confined buckling results in an instability that leads to the nucleation of multiple, oppositely signed RBs, that rapidly propagate away from under the indenter in a wave-like manner [7]. Crucially, upon unloading, they disappear, after dissipating considerable amounts of frictional energy.

In short, our recent work has shown that ripplocations are ubiquitous in nature and span many orders of magnitude in scale. However, since this micromechanism is a new concept at the small-scale in materials, many aspects of their behavior remain little known and opportunities exist to understand their fundamental properties. Therefore, the purpose of this work is to present a number of MD simulation findings of ripplocations in graphite that shed important light on some of their characteristics, specifically their high mobility and interactions with vacancies and remote sources of stress.

Computational details

Atomistic simulations were performed using the LAMMPS software package [21] (lammps.sandia.gov) using the AIREBO interatomic potential [22], which includes both covalent and Van der Waals bonding between C atoms and is therefore well suited to modeling of graphite. The AIREBO potential has previously been used to study deformation of graphite and the properties of vacancies [23].

Unless otherwise specified, all configurations are periodic in the x, y and z, directions, spanning 20 unit cells in the x-axis and 2 unit cells in the periodic y-axis. Typically, the y direction is quite short, about twice the Van der Waals interaction radius. A single layer in a pristine graphite system is compressed by a unit cell, resulting in a periodic system, to produce the ripplocation.

Results

The main results of this work can be found in three movies. Movie 1: In an attempt to obtain the true ground state, a periodic ripplocation underwent repeated cycles of conjugate gradient minimization and 1 ps of low-temperature MD simulation.

Movie 2: In a system with a periodic ripplocation, vacancy clusters were introduced in the same plane, numbering 1, 4 and 8 units per unit cell, the latter two spanning the entire simulation cell in the y-direction. Systems were allowed to evolve through MD at 10 K using an isobaric thermostat.

Movie 3: A ripplocation, periodic in the x- and y-directions, was allowed to evolve at 10 K using an isobaric thermostat as a cylindrical indenter with a radius of 1 nm tangent to the z-direction free surface was moved in the x-direction at a rate of 670 m/s.

Discussion

Effect of temperature

That the excess energy of ripplocations derives from the bending of planes and local intra-layer decohesion, with a fairly large number of constituent atoms, allows for the possibility of many similar potential low energy,

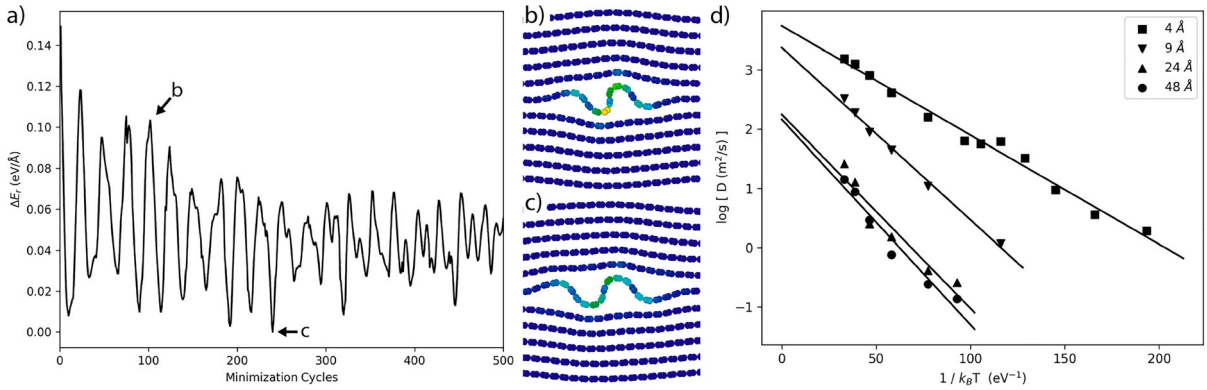

Figure 1. Metastability of ripplocations. (a) Evolution of the energy of a single unconstrained bulk ripplocation while undergoing repeated 1 ps MD and conjugate gradient minimization. Many local energy minima closely spaced in E appear, and the barrier between them is significantly lower than the ripplocation formation energy. Structures at a selected maximum (b) and minimum (c) demonstrate the tradeoff between ripplocation curvature and strain in surrounding layers. (d) Plot demonstrating Arrhenius relationship of observed diffusion coefficients to temperature, from 60 to 350 K, for ripplocation segments of lengths ranging from 4.8 to 48 Å. Activation converges to 32 meV beyond approximately 10 Å after which it is not dependent on segment length.

E, states. The evolution of a single unconstrained ripplocation at 10 K subject to repeated conjugate gradient minimization demonstrated many local energy minima closely spaced in E appear (Figure 1(a)), and the barrier between them is significantly lower than the ripplocation formation energy ($\approx$ 2 eV/Å). Snapshots at the energy minima (Figure 1(b)) and maxima (Figure 1(c)) show the competition between higher-energy buckling and lower-energy long-range strain. The defect also appears to freely move within the plane normal to its line direction. This animated simulation demonstrates significant fluidity, both, in configuration and in motion, remarkably even at 10 K. At higher temperatures, in addition to spontaneous reconfiguration, the ripplocations were significantly mobile. For a short 4.8 Å segment, below 60 K, no clear trend is evident, but at 60 K and above, we observe a clear Arrhenius trend (Figure 1(d)). As the length of the ripplocation increases, the onset of linear behavior occurs at higher temperatures and beyond approximately 10 Å, the activation energy converges to approximately 32 meV. This is substantially lower than the 5.6 meV/Å found from first principles nudged elastic band computations in MoS_2 [8], and does not satisfy a linear scaling relationship with segment length.

Interaction between bulk ripplocations and vacancies

A ripplocation—like an interstitial loop in metals [24,25]—is comprised of local 'excess' material relative to a pristine crystal. This is why it is not surprising that the sub-linear energy scaling of bulk ripplocations with n [9] is reminiscent of interstitial loops' behavior in metals [24,25]. As an interstitial annihilates with a vacancy, our modeling of the interaction of BRs with vacancies indicated that they attract (Movie 2, Figure 2). To demonstrate this aspect a ripplocation is inserted in the proximity of a vacancy or a group of vacancies formed by removing either a single atom (Figure 2(a)), or a row of atoms (Figure 2(b)). In the first case, the ripplocation moves quickly towards the vacancy, its motion arrested when the vacancy occupies a position of high curvature (Figure 2(c)). The total energy of this system is lower than a vacancy in flat graphite by 1.7 eV, with the energy reduction stemming from out-of-plane displacement of vacancy-adjacent atoms. In the second case, the rippled plane unfolds, subducting one end of the layer over the other (Figure 2(d)). In addition to these cases, when a full unit cell is removed, the ripplocation and vacancy annihilate and the perfect crystal is recovered (not shown). The final configuration thus depends on the details of the initial configuration of vacancies near the ripplocation. Prior work studying vacancies in flat graphene [26], as well as with externally imposed curvature [27] have demonstrated the energy reduction of graphene vacancies induced by bending. Here we show that not only are the ripplocations highly mobile, even at 10 K, but that their curvature provides a driving force for attraction. Little work has so far been performed on changes to vacancy migration barriers in the response to curvature or local strain, but it is possible that ripplocations might either encourage or hinder vacancy migration. Due to the relatively low temperatures and time scales for vacancy diffusion, in our simulations the vacancies remain immobile.

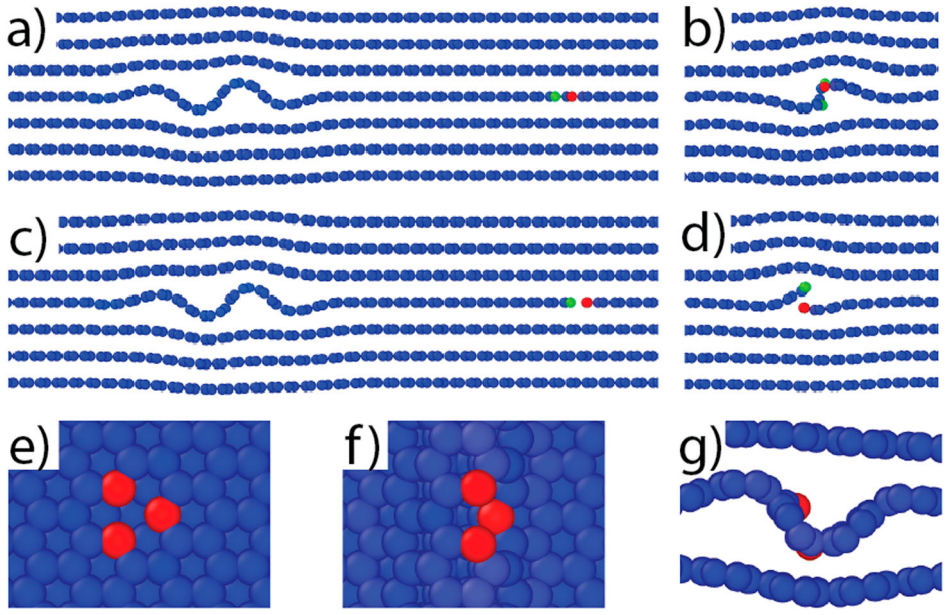

Figure 2. Ripplocation-vacancy interactions. Two configurations of ripplocation-vacancy interactions at 10 K. (a) A ripplocation on the same layer as a single vacancy spontaneously migrates and forms a complex (b) with the vacancy. (c) On the same layer as a broken plane segment, the ripplocation causes one layer to subduct beneath the other (d). The final row shows a top-down (e,f) and side view (g) of the vacancy area. While in the initial configuration (e), the vacancy adjacent atoms remain within the graphene plane, when adjacent to the ripplocation (f, g) they protrude out of plane.

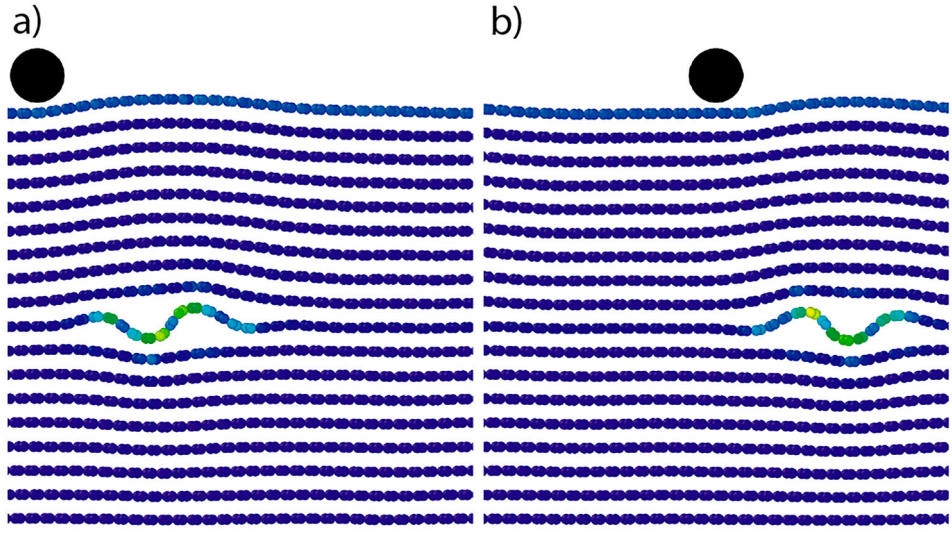

Figure 3. Motion in response to remote stress. (a) An indenter at the left edge of a ripplocation is gradually moved to the right, where is appears to 'push' the ripplocation also to the right (b).

Motion in response to a remote stress

Ripplocations demonstrate response to stress fields induced by indenters in a variety of configurations. When a ripplocation is embedded in a system with a free surface in the {0001} plane, a small section of material is pushed beyond the original free surface. When a 5 Å radius indenter is moved parallel to this surface, as close as possible such that it would not interact with the original terminal plane, it has the appearance of slowly 'pushing' the ripplocation (Figure 3, Movie 3). In this scenario, no indentation stress is directly generated in the immediate vicinity of the ripplocation, but long-range interactions between anisotropic ripplocation strain fields are sufficient to induce motion. It is likely that the fully

reversible stress–strain loops observed when spherical nanoindenters are repeatedly pushed into a surface normal to the basal planes can be attributed to such motion, where the motion and compression of ripplocations are fully reversible and dissipate energy through friction. Evidence that ripplocations are nucleated under a spherical nanoindenter was established in our previous work [9].

Beyond fundamental mechanical properties, ripplocations may also provide an explanation for the response of layered material to irradiation. Buckles and folds in graphene or graphite layers induce a c-axis expansion and a-axis contraction, similar to that observed in bulk graphite induced by neutron irradiation [28]. Recent experimental evidence confirms this effect and demonstrates the presence of folded defects remarkably similar to our simulated predictions [12]. Experiments in the MAX phases demonstrate micron-order denuded zones adjected to grain boundaries [29]. The nucleation of ripplocations and high mobility towards interfaces (e.g. grain boundaries, free surfaces, etc.) and tensile strain fields could explain some of this behavior.

In conclusion, this work suggests a new direction in the analysis of deformation in layered solids. The high mobility and corresponding response to remote force suggests that ripplocations play a key role in the behavior of layered materials. As much of the work performed on layered materials has assumed flat planes with dislocations as the only mechanism of deformation or strain accommodation, some of these results will need to be re-examined. Finally, since ripplocations are a buckling phenomenon, we expect that their relevance does not depend closely on length-scale, but might manifest in any size system with highly anisotropic deformation.

Disclosure statement

No potential conflict of interest was reported by the authors.

Funding

This work was funded by the CMMI division of the National Science Foundation [grant number 1728041].

ORCID

J. Gruber http://orcid.org/0000-0001-8284-0940
M. W. Barsoum http://orcid.org/0000-0001-7800-3517

References

[1] Bell IA, Wilson CJL, McLaren AC, et al. Kinks in mica: role of dislocations and (001) cleavage. Tectonophysics. 1986;127:49–65.
[2] Kronenberg AK, Kirby SH, Pinkston J. Basal slip and mechanical anisotropy in biotite. J Geophys Res 1990;95:19257.
[3] Christoffersen R, Kronenberg AK. Dislocation interactions in experimentally deformed biotite. J Struct Geol. 1993;15:1077.
[4] Mares VM, Kronenberg AK. Experimental deformation of muscovite. J Struct Geol. 1993;15:1061–1075.
[5] Kelly BT. Physics of graphite. London: Applied Science Publishers; 1981.
[6] Hobbs PV. Ice physics. Oxford: Clarendon Press; 1974.
[7] Barsoum MW, Zhao X, Shanazarov S, et al. Ripplocations: a universal deformation mechanism in layered solids. Phys Rev Mater. 2019;3:013602.
[8] Kushima A, Qian X, Zhao P, et al. Ripplocations in van der Waals layers. Nano Lett. 2015;15:1302–1308.
[9] Gruber J, Lang AC, Griggs J, et al. Evidence for bulk ripplocations in layered solids. Sci Rep. 2016;6:33451.
[10] Barsoum MW, Zhen T, Zhou A, et al. Microscale modeling of kinking nonlinear elastic solids. Phys Rev B. 2005;71:134101. doi:10.1103/PhysRevB.71.134101.
[11] Kim K, Lee Z, Malone BD, et al. Multiply folded graphene. Phys Rev B. 2011;83:245433. doi:10.1103/PhysRevB.83.245433.
[12] Johns S, Poulsen T, Kane JJ, et al. Formation of carbon nanostructures in nuclear graphite under high-temperature in situ electron-irradiation. Carbon. 2019; 143:908–914. doi:10.1016/j.carbon.2018.11.077.
[13] Wang W, Chen W, Liu H, Zhang H. Ripplocations, kink bands and delamination cracks in carbon cathode materials. Carbon Lett. 2019. doi:10.1007/s42823-019-00040-0.
[14] Zhang S. Etude de la Réactivité chimique des monocristaux de phase MAX. Grenoble: Université Grenoble Alpes; 2018.
[15] Aslin J, Mariani E, Dawson K. Ripplocations provide a new mechanism for the deformation of phyllosilicates in the lithosphere. Nat Comm. 2019;10:686.
[16] Ganguly S, Das D, Horbach J, et al. Plastic deformation of a permanently bonded network: stress relaxation by pleats. J Chem Phys. 2018;149:184503. doi:10.1063/1.5051312.
[17] Han X, Liu P, Sun D, et al. Quantifying the role of interface atomic structure in the compressive response of Ti2AlN/TiAl composite using MD simulations. J Mater Sci. 2019;54:5536–5550. doi:10.1007/s10853-018-03237-2.
[18] Freiberg D, Barsoum MW, Tucker GJ. Nucleation of ripplocations through atomistic modeling of surface nanoindentation in graphite. Phys Rev Mater. 2018;2. doi:10.1103/PhysRevMaterials.2.053602.
[19] Barsoum MW, Murugaiah A, Kalidindi SR, et al. Kinking nonlinear elastic solids, nanoindentations and geology. Phys Rev Lett. 2004;92:255508–255501.
[20] Barsoum MW, Murugaiah A, Kalidindi SR, et al. Kink bands, nonlinear elasticity and nanoindentations in graphite. Carbon. 2004;42:1435–1445.
[21] Plimpton S. Fast parallel algorithms for short-range molecular dynamics. J Comp Phys. 1995;117:1–19.
[22] Stuart SJ, Tutein AB, Harrison JA. A reactive potential for hydrocarbons with intermolecular interactions. J Chem Phys. 2000;112:6472–6486.

[23] Latham CD, McKenna AJ, Trevethan TP, et al. On the validity of empirical potentials for simulating radiation damage in graphite: a benchmark. J Phys: Condens Matter. 2015;27:316301. doi:10.1088/0953-8984/27/31/316301.
[24] Osetsky YN, Bacon DJ, Serra A, et al. Stability and mobility of defect clusters and dislocation loops in metals. J Nucl Mater. 2000;276:65–77.
[25] Marian J, Wirth BD, Perlado JM. Mechanism of formation and growth of $< 100 >$ interstitial loops in Ferritic materials. Phys Rev Lett. 2002;88:255507.
[26] Rodrigo L, Pou P, Pérez R. Graphene monovacancies: electronic and mechanical properties from large scale ab initio simulations. Carbon. 2016;103:200–208. doi:10.1016/j.carbon.2016.02.064.
[27] Srivastava D, Menon M, Daraio C, et al. Vacancy-mediated mechanism of nitrogen substitution in carbon nanotubes. Phys Rev B. 2004;69:153414. doi:10.1103/PhysRevB.69.153414.
[28] Heggie MI, Suarez-Martinez I, Davidson C, et al. Buckle, ruck and tuck: a proposed new model for the response of graphite to neutron irradiation. J Nucl Mater. 2011;413:150–155. doi:10.1016/j.jnucmat.2011.04.015.
[29] Tallman DJ, He L, Gan J, et al. Effects of neutron irradiation of Ti 3 SiC 2 and Ti 3 AlC 2 in the 121–1085°C temperature range. J Nucl Mater. 2017;484:120–134. doi:10.1016/j.jnucmat.2016.11.016.